# THE EFFECTS OF A POROELASTIC PLATE EXTENSION IN THE SOUND SCATTERING OF A NACA0012 AIRFOIL

**Cristiano Pimenta, cpimenta@fem.unicamp.br**[1]
**William R. Wolf, wolf@fem.unicamp.br**[1]
**André V. G. Cavalieri, andre@ita.br**[2]

[1]Universidade Estadual de Campinas
[1]Instituto Tecnológico de Aeronáutica

***Abstract:*** *The scattering of sound from a NACA0012 airfoil with a poroelastic plate extension is investigated through a numerical methodology. The boundary element method is applied to solve the Helmholtz equation subjected to the boundary conditions associated to the vibration of the plate. The poroelastic plate is considered as a cantilever configuration installed in the trailing edge of a NACA0012 airfoil. A pseudospectral method is implemented to obtain the structural modal basis subjected to the boundary conditions of a clamped-free plate. The modal basis of the plate is then used as a boundary condition to couple the interaction between sound scattering and the structural phenomenon. The scattered sound is produced by a point quadrupole source which represents the sound from a turbulent vortex. Different Helmholtz numbers based on the chord are investigated. A model is employed to represent the effects of perforations in the plate surface. A parametric study is performed for a two-dimensional case where the effects of porosity, elasticity and length of the plate extension is investigated in terms of scattered sound level.*
***Keywords:*** *Aeroacoustic, noise reduction, sound-structure interaction*

## 1. INTRODUCTION

In nature, many owls species can eliminate for some range of frequency the noise generated during flight. The noise reduction is related with specific properties of the owls's wing, such as, porosity and elasticity. Recently,Jaworski and Peake (2013) performed a theoretical analysis of the scattered sound from a poroelastic edge combining the effects of the porosity and elasticity for a semi-finite plate. The analytical results shown by Jaworski and Peake (2013) is for high frequency regime, due the assumption of semi-infinite plate made. Cavalieri *et al.* (2014) developed a novel framework to perform a numerical analysis of the scattered sound for a poroelastic plate with finite chord and infinite span. Results showed that both porosity and elasticity of the plate reduce the scattered sound level, in agreement with previous work considering semi-infinite plate. To investigate the effect of the edges of the plate, Wolf and Cavalieri (2015) developed a new numerical framework to obtain the acoustic scattering by fully three-dimensional poroelastic plates with finite chord and span. More recently, Ayton (2016) presented a theoretical formulation to investigate the scattered sound by a finite rigid plate with a poroelastic plate extension and showed the potential of noise reduction to apply properties inspired in owls wings.

In this work a numerical analysis is performed to compute the scattered acoustics by a NACA 0012 with a poroelastic plate extension. The model analysed is illustrated by Fig. 1 and it is used to investigate the scattering of a point quadrupole source, $S$, by a NACA 0012 with a poroelastic plate extension. The source is excited at high and low Helmholtz numbers $k_0$ based on the chord length, as shown in Fig. 1. The goals of this effort are to extend beyond the numerical work of Cavalieri *et al.* (2016) to evaluate the effect of the poroelastic plate as an extension of a NACA 0012. A parametric study of the plate extension length ($L$) is performed, where the length $L$ is based on the chord of the NACA 0012.

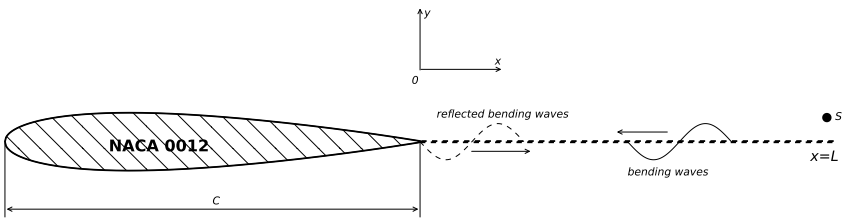


Figure 1: The model problem for an arbitrary source, S.

## 2. MATHEMATICAL MODELLING

The system of equations that model the coupled problem is composed by the Helmholtz equation to obtain the scattered sound, the equation for the plate vibration at the fluid-solid interface, and the linearised Euler equation to relate the pressure at the plate surface and the fluid displacement. The non-dimensional equations following the nondimensionalization proposed by Cavalieri *et al.* (2016), and it can be written in the following way

$$\nabla^2 p + k_0^2 p = -S, \tag{1}$$

$$(1-\alpha_H)\,\nabla^4\eta - \frac{k_0^4}{\Omega^4}\eta = (1+\alpha_H K_R)\,\frac{\epsilon}{\Omega^6}k_0^3\Delta p, \tag{2}$$

$$(1-\alpha_H)\,k_0^2\eta - \frac{\alpha_H K_R}{2R}\Delta p = \left.\frac{\partial p}{\partial y}\right|_{y=0}. \tag{3}$$

The acoustic problem is represented by Eq. (1) where $k_0$ is the acoustic wavenumber and $S$ is the acoustic source function. The boundary conditions for the scattered sound are given by Eq. (2) matching the velocities of the fluid and displacement of the plate at the fluid-structure interface for a perforated elastic plate. To couple the structure and scattering phenomenon Eq. (3) is applied. The constants $\alpha_H$, $R$, $K_R$ are properties of the porous plate and they represent the open area fraction, the pore radius and the Rayleigh conductivity, respectively. For circular apertures, the Rayleigh conductivity is considered as $K_R = 4/\pi$ (Cavalieri *et al.*, 2016). The parameters $\epsilon$ and $\Omega$ are the fluid loading and the vacuum bending wave Mach number. The fluid loading parameter $\epsilon$ depends of the fluid and the plate properties (Howe, 1998). The analysis of the structural-acoustic interaction is governed by three parameters: $\epsilon$, $\Omega$ and $k_0$.

Following the procedure from Cavalieri *et al.* (2016) the solution of the problem using structural modal basis consists in solving an eigenvalue problem subject to the same boundary conditions, and the solution forms a complete orthonormal basis $\phi_i$, such that

$$\nabla^4\phi_i = \beta^4\phi_i, \quad where \quad \langle\phi_i,\phi_j\rangle = \delta_{ij}. \tag{4}$$

In Eq. (4), $\beta$ is the bending wavenumber of the vibration mode $\phi_i$ of the plate. The displacement of the plate $\eta$ is represented by the modal basis, so we can write the displacement as

$$\eta = \sum_i a_i\phi_i. \tag{5}$$

Using Eq. (4) and Eq. (5), the pressure in the transverse direction evaluated at the plate surface through Eq. (3) can be rewritten as (Cavalieri *et al.*, 2016)

$$\left.\frac{\partial p}{\partial y}\right|_{y=0} = (1+\alpha_H K_R)\,\frac{\epsilon k_0^5}{\Omega^6}\sum_j^M\left[\frac{\langle\Delta p,\phi_j\rangle}{\beta_j^4 - \frac{k_0^4}{(1-\alpha_H)\Omega^4}}\right] - \frac{\alpha_H K_R}{2R}\Delta p. \tag{6}$$

Equation (6) relates the vibration problem with the transverse pressure gradient at the plate surface. To solve the Helmholtz equation for the acoustic problem the boundary element method is employed, where $p$ and $\partial p/\partial y|_{y=0}$ need to be solved for. Therefore, Eq. (6) couples the structural-acoustic interaction. It is important to highlight that the formulation can be used to solve the problem of a perforated elastic plate. The particular case of a perforated rigid plate can be obtained considering $\epsilon = 0$ and, for an impermeable elastic plate, considering $\alpha_H = 0$.

## 3. NUMERICAL METHODS

The methodology employed to solve the system of equations for the structural-acoustic interaction requires two different numerical methods.

### 3.1 Boundary element method

The acoustic scattering problem is solved using a boundary element method (BEM)where a point quadrupole source is placed near the trailing edge of the plate. Equation (1) can be rewritten to represent the pressure on the surface induced by the concentrated point source in a quiescent medium,

$$\nabla^2 p(x) + k_0^2 p(x) = -S_i. \tag{7}$$

In Eq. (7), $S_i$ represents the source strength. A quadrupole source models the incident acoustic field and represents the noise generation from a compact turbulent eddy (Cavalieri *et al.*, 2016). A solution for the Helmholtz equation consists in the free space Green's function, $G(x,y)$, which for a two dimensional formulation is given as

$$G(x,y) = \frac{i}{4}H_0^{(1)}\left(k_0|x-y|\right), \tag{8}$$

where $H_0^{(1)}$ is the Hänkel function of the first kind and order zero. The incident quadrupole source can be computed as the second derivative of the Green's function.

From Green's second identity, the boundary integral equation can be written as

$$T(x)p(x) = \int_\Gamma \left[ \frac{\partial p(y)}{\partial n_y} G(x,y) - \frac{\partial G(x,y)}{\partial n_y} p(y) \right] d\Gamma - \frac{\partial^2 G(x,z_i)}{\partial z_{i_m} \partial z_{i_n}} S(z_i) \tag{9}$$

where $T(x) = 0.5$ when $x$ is in a smooth boundary surface $\Gamma$, and $T(x) = 1.0$ when x is any point of the fluid. In the BEM formulation, the scattering surface is discretized into a finite number of elements with length $\Gamma$. The present convention employs **n** as an inward normal vector pointing from the boundary surface to the solid object. The incident source is located in $z_i$.

To obtain the solution of the scattered sound, Eq. (9) must be solved twice. First, we compute the pressure on the boundary surface induced by the incident source and, then, we compute the sound scattered at the far field observer. Notice that Eq. (9) has the term $\partial p/\partial n$ where the structural and acoustic problems are coupled.

### 3.2 Pseudo-spectral method

The structural problem represented by Eq. (2) consists in solving an eigenvalue problem, Eq. (4), to obtain the modal basis of the vibration of the plate. In the present work, for a two dimensional formulation, the Euler-Bernoulli beam model is used. The development from an elementary level of a beam model can be found in DasGupta and Hagedorn (2007). Considering a beam clamped at the trailing edge of NACA 0012 at $x = 0$ and free at the end at $x = L$, we shall apply the following boundary conditions,

$$\eta(0) = 0 \tag{10a}$$

$$\eta'(0) = 0 \tag{10b}$$

$$\eta''(L) = 0 \tag{10c}$$

$$\eta'''(L) = 0. \tag{10d}$$

To solve Eq. (4) subjected to the boundary conditions from Eqs. (10a) - (10d) the pseudo-spectral method is employed to achieve spectral accuracy. Spectral methods are employed for the spatial discretization of partial differential equations and, in general, their general form can be written as suggested by Boyd (2001)

$$\eta(x_i) \cong \sum_{n=\infty}^{N} a_n . \phi_n(x_i), \tag{11}$$

where $\phi_n$ is the basis function and $a_n$ represents the coefficients. For periodic boundary conditions it is common to use Fourier Spectral Methods with exact derivatives for the approximation. Otherwise, for non periodic boundary conditions, the pseudo-spectral or the collocation method are used where the approximation must be exact on the grid points (Boyd, 2001).

The pseudo-spectral method is applied as an interpolatory method for an unknown function $\eta(x_i)$ which requires that the interpolant at each of a set of grid points $\{x_i\}$ gives zero residual. We use the Chebyshev Gauss-Lobatto formula for the interpolation points Boyd (2001) which can be written as

$$x_i = \cos\left(\frac{\pi i}{N}\right), \quad i = 0, 1, \ldots, N \quad with \quad x \in [-1, 1]. \tag{12}$$

In current work, the interpolant uses Lagrange polynomials (delta function) based on the grid points $\{x_i\}$ and the Chebyshev differentiation matrix(D) is used to approximate the derivatives following the procedure developed by Trefethen (2000).

The Chebyshev differentiation matrix is written as $D_N^1 = \partial/\partial x$, where $N$ is the number of grid points and "1" represents the first devirative. The major advantage of this formulation presented by Trefethen (2000) is that we can compute the second derivative via $D_N^2 = D_N^1 \cdot D_N^1$, the square of $D_N$. The discretization of Eq. (4) can be then written as follows

$$D^4\eta = \beta^4\eta, \tag{13}$$

where the differentiation matrix leads to a fourth order differential operator. In this case, rounding errors can affect the approximation when the number of grid points $N$ is increased. Don and Solomonoff (1997) investigated the accuracy of the Chebyshev collocation method for higher derivatives, and computing fourth order derivative and N large can result in very large roundoff error. The alternative is to reduce Eq. (4) to a system of differential equations following the procedure by Cavalieri *et al.* (2016), defining auxiliary variables as

$$w_1 = \eta \tag{14a}$$

$$w_2 = \eta'' \tag{14b}$$

To obtain Eq. (4) in matrix form one has

$$\begin{bmatrix} D^2 & I \\ 0 & D^2 \end{bmatrix} \begin{Bmatrix} w_1 \\ w_2 \end{Bmatrix} = \beta^4 \begin{bmatrix} 0 & 0 \\ I & 0 \end{bmatrix} \begin{Bmatrix} w_1 \\ w_2 \end{Bmatrix}. \tag{15}$$

The same way, the boundary conditions Eqs. (10a) - (10d) can be rewritten as a function of the auxiliary variables $w_1$ and $w_2$. Therefore,

$$\eta(0) = w_1(0) = 0 \tag{16a}$$

$$\eta'(0) = w_1'(0) = D^1\big|_{x=0} = 0 \tag{16b}$$

$$\eta''(L) = w_2(L) = 0 \tag{16c}$$

$$\eta'''(L) = w_2'(L) = D^1\big|_{x=L} = 0. \tag{16d}$$

It is clear that the reduction of the fourth order differential equation to a second order improves the accuracy of the approximation, eliminating the rounding errors of differentiation matrix.

Boundary conditions Eqs. (16a) - (16d) are imposed in Eq. (15) replacing the corresponding lines of the matrix in the left-hand side and the lines of the right-hand side are zeroed. Boundary conditions for the clamped and the free end of the beam are imposed by $w_1$ and $w_2$, respectively. For the vibration problem, the eigenvalue generalized problem is solved to obtain the modal basis of the beam. We have employed a discretization with 320 Chebyshev points. The solution provides values of the bending wavenumber and the modes of vibration of the beam on the Chebyshev grid points $\{x_i\}$. To obtain the modes of vibration on the grid points with locations chosen to be appropriate for the application of the boundary element method, the barycentric interpolation is applied at the grid points $\{x_i\}$ of $N$ points following Berrut and Trefethen (2004).

## 4. RESULTS

In this present work, we obtained the radiated sound by a quadrupole source point of intensity unity placed at $(x, y) = (L, 0.004)$. We calculate the porosity and elasticity effects in acoustic scattering and shown directivity results for observers in the acoustic far-field located 50 chords from the NACA 0012 trailing edge. We have chosen $\epsilon = 0.0021$ as representative of an aluminium plate in air Howe (1998), for NACA 0012 or rigid plate extension we used $\epsilon = 0$. For all cases analysed, one hundred of the bending wavenumber and modes of vibration are used. The numerical simulations used 801 boundary elements in NACA 0012, 801 boundary elements for plate extension with $L = 1c$, 401 boundary elements for plate extension with $L = 0.5c$ and 201 boundary elements for plate extension with $L = 0.25c$.

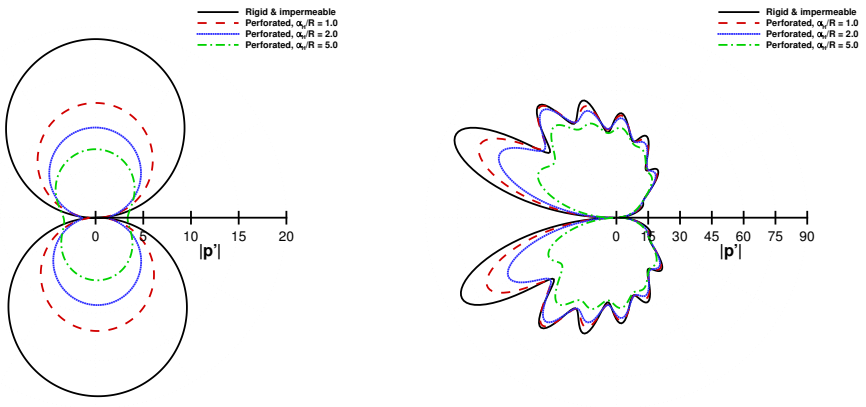


(a) (b)

Figure 2: **Directivities for perforated rigid plate extension with $L = 1c$, (a) $k_0 = 0.1$ and (b) $k_0 = 10$.**

For a perforated rigid plate extension, we take $K_R = 4/\pi$ and evaluate the effects of $\alpha_H/R$ and Helmholtz number $k_0$ on the radiated sound. Figure 2 presents directivity standards for compact and non-compact perforated plate. For lower $k_0 = 0.1$, the results shown by Fig. 2a, the directivity shape changes progressively from a dipole shape to the monopole shape with increasing $\alpha_H/R$, in agreement with theoretical analysis performed by Williams (1972). For higher $k_0 = 10$, the results of directivity shape changes from a lobed cardioid to the dipole shape with the increasing $\alpha_H/R$ as shown by Fig. 2b. The effect of porosity on sound radiation is more efficient for lower $k_0$ as shown by Fig. 2

For an impermeable elastic plate extension, we take $\alpha_H = 0$ and evaluate the effects of parameters $\Omega$ and Helmholtz number $k_0$ on the radiated sound. The bending stiffness of the plate is related with $\Omega$, and reductions of the stiffness lead

to lower $\Omega$. Figure 3 presents directivity standards for compact and non-compact elastic plate. For lower $k_0 = 0.1$ the directivity dipole shape is preserved for any $\Omega$ and the effect of elasticity on sound radiation is less effective than porosity, as shown by Fig. 3a. Otherwise, for higher $k_0 = 10$ the directivity shape changes from a lobed cardioid to the dipole shape, as seen in Fig. 3b, and the effect of elasticity on sound radiation is more effective than porosity.

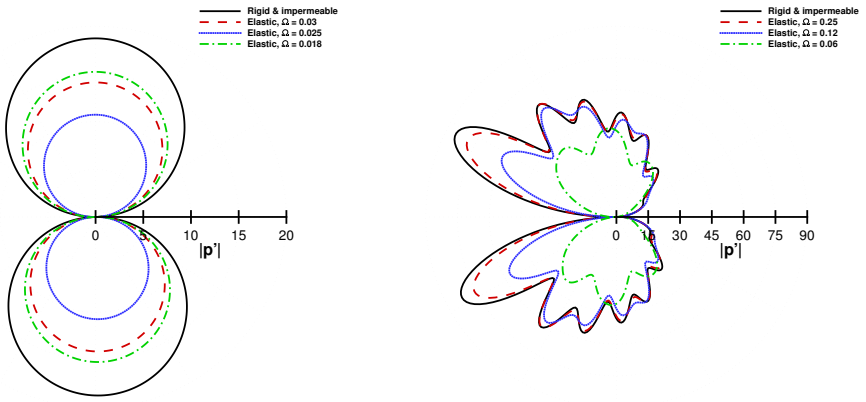


(a) (b)

Figure 3: **Directivities for impermeable elastic plate extension with $L = 1c$, (a) $k_0 = 0.1$ and (b) $k_0 = 10$.**

As discussed previously, the effects of porosity and elasticity are opposites on sound radiation as $k_0$ increases. The combination of the porosity and elasticity may be a potential way to reduce scattered sound for both lower $k_0$ and higher $k_0$. For a perforated elastic plate extension, we chosen to fix $\alpha_H/R = 2.0$ and evaluate the effects of varying $\Omega$ and Helmholtz number $k_0$ on the radiated sound. Figure 4 presents directivity standards for compact and non-compact perforated elastic plate. For lower $k_0 = 0.1$ the directivity shape tend to changes from a dipole shape to the monopole shape, as shown by Fig. 4a, due the combination of both properties porosity and elasticity this transition is slow. For higher $k_0 = 10$ the directivity shape changes from a lobed cardioid to the dipole shape, as seen in Fig. 4b. We observed the combined effects of porosity and elasticity lead to more significant reductions of the radiated sound for lower $k_0$ and higher $k_0$.

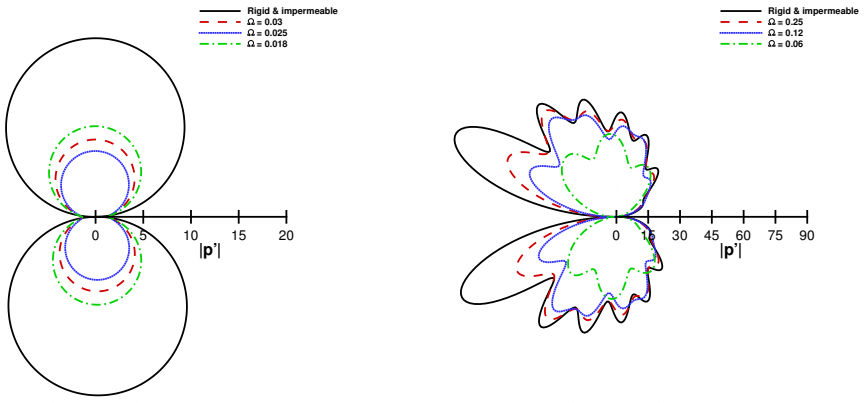


(a) (b)

Figure 4: **Directivities for perforated elastic plate extension with $L = 1c$, varying $\Omega$ for $\alpha_H/R = 2.0$, (a) $k_0 = 0.1$ and (b) $k_0 = 10$.**

A parametric study of the length plate extension $L$ was performed to evaluate the impact of the combined effects of porosity and elasticity on sound radiation. Figure 5 presents the directivities shape for three different lengths of the plate extension $L$ for lower $k_0$. It turned out that lower length of the plate extension, diminished the combined effects of porosity and elasticity in noise reduction. The length of the plate extension $L$ changes the bending wavenumbers of the modal basis, decreasing the effect of the elasticity, as shown by Fig. 5. For a small lengths $L$ the reduction of the radiated sound is due a porosity, as seen in Fig. 5a, in this case the elasticity does not affect the results.

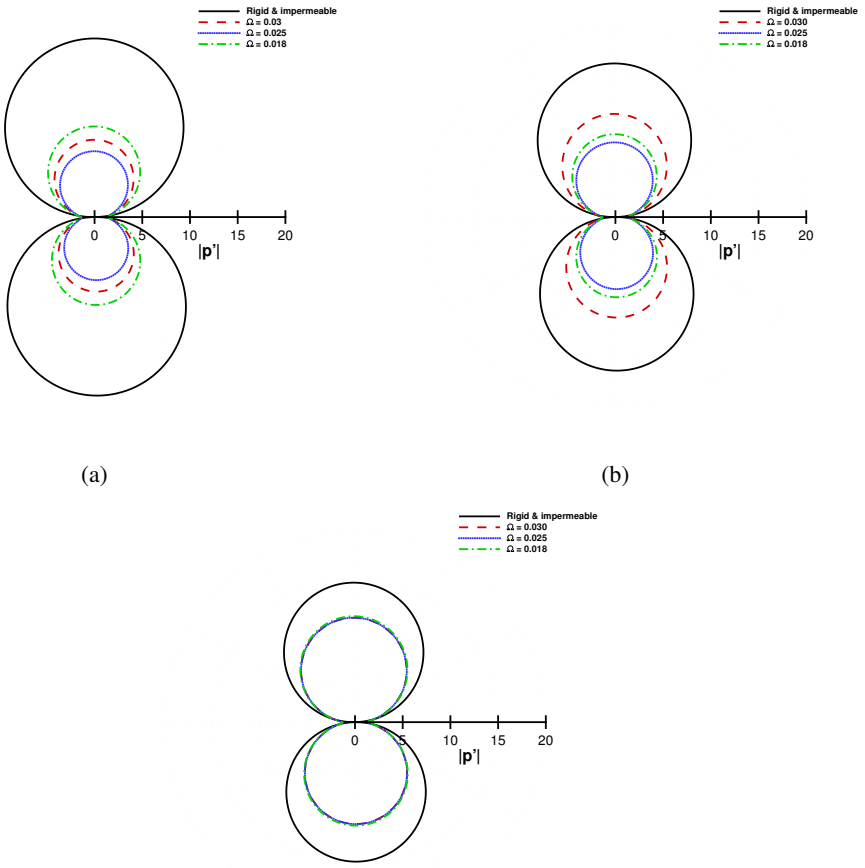


(a) (b)

(c)

Figure 5: **Directivities for perforated elastic plate with different extensions, varying $\Omega$ for $\alpha_H/R = 2.0$ and $k_0 = 0.1$, (a) $L = 1c$, (b) $L = 0.5c$ and (c) $L = 0.25c$.**

Figure 6 presents the directivities shape for three different lengths of the plate extension $L$ for higher $k_0$. We observed the same results, the length of the plate extension affects the elasticity benefits and the reduction on sound radiation is due the porosity, as shown by Fig. 6c.

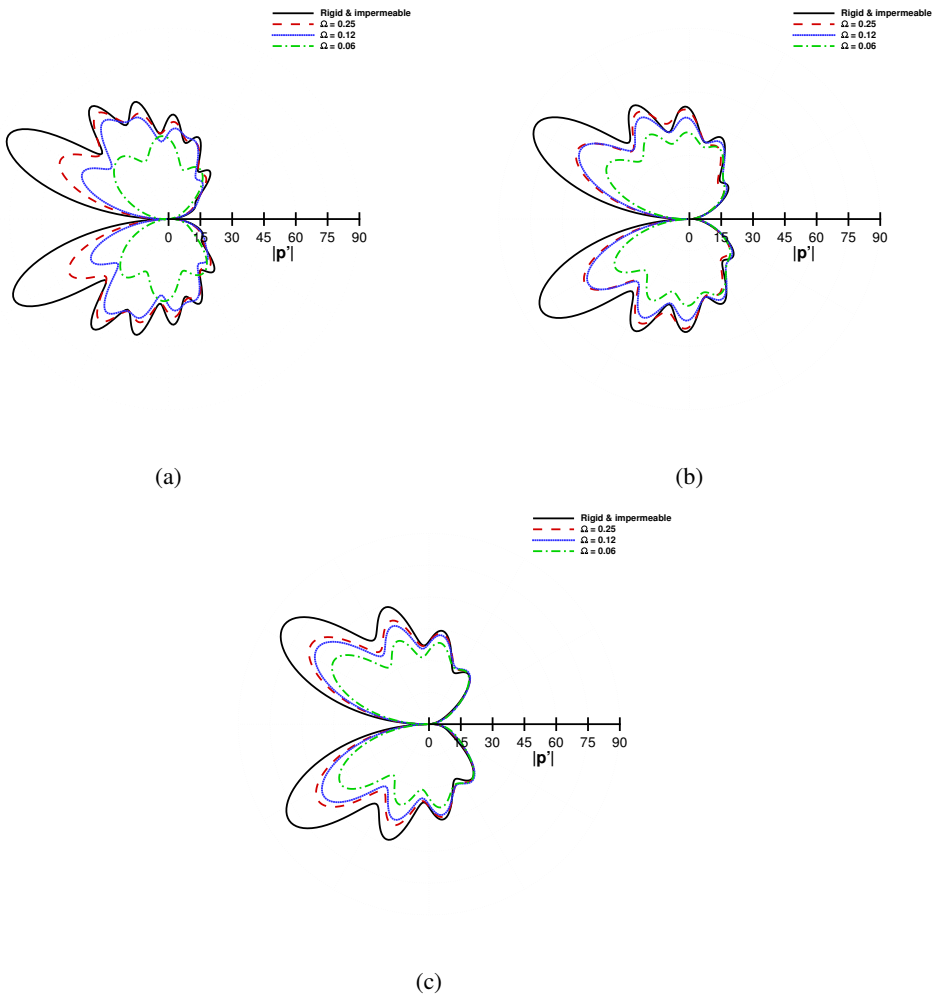


Figure 6: **Directivities for perforated elastic plate with different extensions, varying $\Omega$ for $\alpha_H/R = 2.0$ and $k_0 = 10.0$, (a) $L = 1c$, (b) $L = 0.5c$ and (c) $L = 0.25c$.**

## 5. CONCLUSIONS

In this work, we present a two-dimensional numerical formulation to obtain the acoustic-structural interaction and compute the acoustic scattered by NACA 0012 with a poroelastic plate extension. The modal basis of free-vibration problem is obtained applying pseudo-spetral method subjected to the boundary conditions, clamped at the trailing edge of NACA 0012 and free at end of the plate. The boundary element formulation is employed to solve Helmholtz equation. The modes of vibration computed by pseudo-spectral method is interpolated into boundary element mesh. The effects of porosity and elasticity lead to reductions of the radiated sound when compared to the rigid and impermeable plate. We see that for lower $k_0$ porosity is more efficient in reducing the radiated sound compared with elasticity effects. Otherwise, for higher $k_0$ elasticity is more efficient in reducing the radiated sound compared with porosity effects. A optimum solution to reduce scattered sound can be achieved by the combination of the porosity and elasticity for lower and higher $k_0$. We investigated in this present work, the length extension $L$ of the poroelastic plate. For small length extension the elasticity effects does not affect the reduction of radiated sound. Thus, poroelastic extension plate is a promising solution to reduce trailing-edge noise, but is important to have length extension sufficiently to gain the both benefits porosity and elasticity.

## 6. ACKNOWLEDGEMENTS

The authors gratefully acknowledge the partial support for this research provided by Conselho Nacional de Desenvolvimento Científico e Tecnológico, CNPq, under the Research Grant No. 470695/2013-7. The first author is supported by a CAPES MSc. scholarship, which is also acknowledged.

## 7. REFERENCES

Ayton, L.J., 2016. "Acoustic scattering by a finite rigid plate with a poroelastic extension". *Journal of Fluid Mechanics*, Vol. 791, pp. 414–438.

Berrut, J.P. and Trefethen, L.N., 2004. "Barycentric lagrange interpolation". *Siam Review*, Vol. 46, No. 3, pp. 501–517.

Boyd, J.P., 2001. *Chebyshev and Fourier spectral methods*. Courier Corporation.

Cavalieri, A.V.G., Wolf, W.R. and Jaworski, J.W., 2016. "Numerical solution of acoustic scattering by finite perforated elastic plates". *Proceedings of the Royal Society of London A: Mathematical, Physical and Engineering Sciences*, Vol. 472, No. 2188.

Cavalieri, A.V., Wolf, W.R. and Jaworski, J.W., 2014. "Acoustic scattering by finite poroelastic plates". In *20th AIAA/CEAS Aeroacoustics Conference*. p. 2459.

DasGupta, A. and Hagedorn, P., 2007. "Vibrations and waves in continuous mechanical systems".

Don, W.S. and Solomonoff, A., 1997. "Accuracy enhancement for higher derivatives using chebyshev collocation and a mapping technique". *SIAM Journal on Scientific Computing*, Vol. 18, No. 4, pp. 1040–1055.

Howe, M.S., 1998. *Acoustics of fluid-structure interactions*. Cambridge university press.

Jaworski, J.W. and Peake, N., 2013. "Aerodynamic noise from a poroelastic edge with implications for the silent flight of owls". *Journal of Fluid Mechanics*, Vol. 723, pp. 456–479.

Trefethen, L.N., 2000. *Spectral methods in MATLAB*, Vol. 10. Siam.

Williams, J.E.F., 1972. "The acoustics of turbulence near sound-absorbent liners". *Journal of Fluid Mechanics*, Vol. 51, pp. 737–749.

Wolf, W.R. and Cavalieri, A.V., 2015. "A fast numerical framework for acoustic scattering by 3d poroelastic plates". In *21st AIAA/CEAS Aeroacoustics Conference*. p. 3260.

## 8. RESPONSIBILITY NOTICE

The following text, properly adapted to the number of authors, must be included in the last section of the paper: The author(s) is (are) the only responsible for the printed material included in this paper.